The Λ(1405) state in a chiral unitary approach with off-shell corrections to dimensional regularized loop functions

Fang-Yong Dong(董方勇)[1] Bao-Xi Sun(孙宝玺)[1,2] Jing-Long Pang(庞景龙)[2]

[1] College of Applied Sciences, Beijing University of Technology, Beijing 100124, China
[2] Department of Physics, Peking University, Beijing 100871, China

Abstract: The Bethe-Salpeter equation is solved in the framework of the unitary coupled-channel approximation by using the pseudoscalar meson-baryon octet interaction. The loop function of the intermediate meson and baryon is deduced in a dimensional regularization scheme, where the relativistic kinetic effect and off-shell corrections are taken into account. Based on the experimental data at the K^-p threshold, the subtraction constants in the loop function are determined. The squared amplitude is suppressed strongly and only one Λ(1405) state is generated dynamically in the strangeness $S=-1$ and isospin $I=0$ sector.

Keywords: chiral lagrangian, kaon-baryon interaction, hyperon

PACS: 12.39.Fe, 13.75.Jz, 14.20.Jn **DOI:** 10.1088/1674-1137/41/7/074108

1 Introduction

There are some different views about the structure of Λ(1405), and its structure has been challenging the standard view of baryons made of three quarks for decades. Some theorists think that the Λ(1405) could be a kind of molecular state arising from the interaction of the πΣ and $\bar{K}N$ channels [1–3]. Furthermore, the number of poles in the complex energy plane is also a puzzle for the Λ(1405) resonance. Some people predict that one pole corresponds to the Λ(1405) resonance [1, 4, 5], while the calculation results in the unitary coupled-channel approximation show there are two poles in the 1400 MeV region [6–10]. Two Λ(1405) states were claimed for the first time in Ref. [6], explained as combinations of a single state and a octet state when the $SU(3)$ symmetry breaks up [7]. It is reported that only one resonance state is observed around 1400 MeV [11–14]. However, in a modern $K^+\Sigma\pi$ photoproduction experiment by the CLAS Collaboration, some signature effects for a two-pole picture of the isospin $I=0$ Λ(1405) have been found [15].

In the past few years, the energy shift and width of the 1s state of kaonic hydrogen have been measured precisely at the SIDDHARTA experiment at $DA\Phi NE$ [16], providing a constraint on the determination of parameters in the unitary coupled-channel approximation. The new experimental data have stimulated theoretical studies of the kaon-nucleon interaction and the properties of the Λ(1405) particle [17–20], where the Bethe-Salpeter equation is solved in the unitary coupled-channel approximation, and the two-pole picture of the Λ(1405) particle is stressed. A direct comparison of the most recent approaches is made in Ref. [21]. However, a loop function of the meson and the baryon in the on-shell factorization is used when the Bethe-Salpeter equation is solved, and some important elements might be eliminated in this approximation, which would result in the uncertainty of the calculation. In this article, we calculate the loop function in a dimensional regularization scheme, and then solve the Bethe-Salpeter equation in the unitary coupled-channel approximation.

This manuscript is organized as follows. In Section **2**, the framework of the unitary coupled-channel approximation is discussed. In particular, the loop function of the pseudoscalar meson and the baryon octet is obtained in the dimensional regularization. In Section **3**, the parameters in the unitary coupled-channel approximation are determined according to the experimental data at the K^-p threshold. In Sections **4** and **5**, the cases with isospin $I=0$ and $I=1$ are calculated, respectively. Some discussion and a conclusion are given in Section **6**.

2 Framework

The lowest order meson-baryon chiral Lagrangian is given as [22–24]

$$L=\langle\bar{B}i\gamma^\mu\frac{1}{4f^2}[(\Phi\partial_\mu\Phi-\partial_\mu\Phi\Phi)B-B(\Phi\partial_\mu\Phi-\partial_\mu\Phi\Phi)]\rangle, \quad (1)$$

where the symbol $\langle\cdots\rangle$ denotes the trace of a matrix in $SU(3)$ space. The matrices of the pseudoscalar meson

Received 14 November 2016, Revised 3 April 2017

©2017 Chinese Physical Society and the Institute of High Energy Physics of the Chinese Academy of Sciences and the Institute of Modern Physics of the Chinese Academy of Sciences and IOP Publishing Ltd

and the baryon octet are given as follows:

$$\Phi=\begin{pmatrix}\frac{1}{\sqrt{2}}\pi^0+\frac{1}{\sqrt{6}}\eta & \pi^+ & K^+\\ \pi^- & -\frac{1}{\sqrt{2}}\pi^0+\frac{1}{\sqrt{6}}\eta & K^0\\ K^- & \bar{K}^0 & -\frac{2}{\sqrt{6}}\eta\end{pmatrix} \quad (2)$$

and

$$B=\begin{pmatrix}\frac{1}{\sqrt{2}}\Sigma^0+\frac{1}{\sqrt{6}}\Lambda & \Sigma^+ & p\\ \Sigma^- & -\frac{1}{\sqrt{2}}\Sigma^0+\frac{1}{\sqrt{6}}\Lambda & n\\ \Xi^- & \Xi^0 & -\frac{2}{\sqrt{6}}\Lambda\end{pmatrix}. \quad (3)$$

Ten coupled channels are considered in the case of pseudoscalar meson-baryon octet scattering processes in the low energy region. These are: K^-p, $\bar{K}^0n$, $\pi^0\Lambda$, $\pi^0\Sigma^0$, $\pi^+\Sigma^-$, $\pi^-\Sigma^+$, $\eta\Lambda$, $\eta\Sigma^0$, $K^+\Xi^-$ and $K^0\Xi^0$ [7].

The potential of the baryon octet and the pseudoscalar meson can be obtained from the lowest order meson-baryon chiral Lagrangian in Eq. (1), and can be written as

$$V_{ij}=-C_{ij}\frac{1}{4f^2}\bar{U}(p_2)\gamma_\mu U(p_1)(k_1^\mu+k_2^\mu), \quad (4)$$

where p_1, p_2 (k_1, k_2) are the initial and final momenta of the baryons (mesons), respectively. In the case of low energies, the three-momenta of the baryons and mesons can be neglected, and thus only the γ^0 component is relevant, i.e.,

$$\bar{U}(p_2)\gamma_\mu U(p_1)\approx\left(\frac{M_i+E}{2M_i}\right)^{\frac{1}{2}}\left(\frac{M_j+E'}{2M_j}\right)^{\frac{1}{2}}, \quad (5)$$

where M_i and M_j denote the initial and final baryon masses, respectively, while E and E' stand for the initial and final baryon energies in the center of mass frame, respectively. The spin orientation of the initial baryon is the same as that of the final baryon. Moreover,

$$k_1^0+k_2^0\approx 2\sqrt{s}-M_i-M_j, \quad (6)$$

with $\sqrt{s}$ the total energy of the system in the center of mass frame.

Therefore, if and only if the external particles are all on-shell, the potential in Eq. (4) takes a simple form as follows [7]:

$$V_{ij}=-C_{ij}\frac{1}{4f^2}(2\sqrt{s}-M_i-M_j)\left(\frac{M_i+E}{2M_i}\right)^{\frac{1}{2}}\left(\frac{M_j+E'}{2M_j}\right)^{\frac{1}{2}}, \quad (7)$$

where the coefficient C_{ij} is shown in Table B1, and the decay constant $f=1.123f_\pi$ [9] with the pion decay constant $f_\pi=92.4$ MeV.

The scattering amplitude can be constructed by solving the Bethe-Salpeter equation

$$\begin{aligned}T(p_1,k_2;p_2,k_2) &= V(p_1,k_2;p_2,k_2)+i\int\frac{\mathrm{d}^4q}{(2\pi)^4}V(p_1,k_1;q,p_1+k_1-q)S(q)\Delta(p_1+k_1-q)T(q,p_1+k_1-q;p_2,k_2)\\ &= V(p_1,k_2;p_2,k_2)+i\int\frac{\mathrm{d}^4q}{(2\pi)^4}V(p_1,k_1;q,p_1+k_1-q)S(q)\Delta(p_1+k_1-q)V(q,p_1+k_1-q;p_2,k_2)+\cdots, \quad (8)\end{aligned}$$

where the propagators of the intermediate baryon and meson can be written as $iS(q)=i/(\not{q}+M_l+i\varepsilon)$ and $i\Delta(p_1+k_1-q)=i/[(p_1+k_1-q)^2-m_l^2+i\epsilon]$, respectively [25]. If the potential $V(p_1,k_1;q,p_1+k_1-q)$ in Eq. (8) is divided into an on-shell part and an off-shell part, the off-shell part of the potential $V(p_1,k_1;q,p_1+k_1-q)$ should be proportional to the on-shell part, and can be absorbed into the on-shell part of the potential if a suitable renormalization of coupling constants is performed. Therefore, only the on-shell part of the potential of the baryon and the meson needs to be taken into account when the Bethe-Salpeter equation is solved. Thus the Bethe-Salpeter equation in Eq. (8) is simplified as

$$T=V+VGT, \quad (9)$$

or

$$T=[1-VG]^{-1}V, \quad (10)$$

where the loop function of a baryon and a meson G is a diagonal matrix, i.e., $G_{ln}=G_l\delta_{ln}$, and the diagonal element G_l can be written as

$$G_l=i\int\frac{\mathrm{d}^4q}{(2\pi)^4}\frac{\not{q}+M_l}{q^2-M_l^2+i\epsilon}\frac{1}{(P-q)^2-m_l^2+i\epsilon}, \quad (11)$$

with $P=p_1+k_1$ the total momentum of the system, m_l the meson mass, and M_l the baryon mass, respectively. More detailed discussion on how to transform the Bethe-Salpeter equation from an integral form to an algebra form can be found in Refs. [25, 26].

In Ref. [26], the loop function G in Eq. (11) is calculated numerically by setting the maximum three-momentum $q_{\max}$, which is called the momenum cut-off method. However, in Ref. [6], a dimensional regularization form of the loop function G is deduced with the on-shell approximation

$$\not{q}+M_l=2M_l, \quad (12)$$

which is valid only when it is applied to the Dirac spinor $U(q)$.

In the on-shell factorization approximation, the loop

function is denoted as

$$\begin{aligned} G_l'(s) &= i\int\frac{\mathrm{d}^d q}{(2\pi)^4}\frac{2M_l}{q^2-M_l^2+i\epsilon}\frac{1}{(P-q)^2-m_l^2+i\epsilon} \\ &= \frac{2M_l}{16\pi^2}\left\{a_l+\ln\frac{M_l^2}{\mu^2}+\frac{m_l^2-M_l^2+s}{2s}\ln\frac{m_l^2}{M_l^2}\right. \\ &\quad +\frac{\bar{q}_l}{\sqrt{s}}\big[\ln(s-(M_l^2-m_l^2)+2\bar{q}_l\sqrt{s}) \\ &\quad +\ln(s+(M_l^2-m_l^2)+2\bar{q}_l\sqrt{s}) \\ &\quad +\frac{\bar{q}_l}{\sqrt{s}}-\ln(-s+(M_l^2-m_l^2)+2\bar{q}_l\sqrt{s}) \\ &\quad \left.-\ln(-s-(M_l^2-m_l^2)+2\bar{q}_l\sqrt{s})\big]\right\}, \end{aligned} \tag{13}$$

with μ=630 MeV the scale of dimensional regularization and the symbol a_l the subtraction constant.

In Eq. (13), $\bar{q}_l$ denotes the three-momentum of the meson or the baryon in the center of mass frame and is given by

$$\bar{q}_l=\frac{\lambda^{1/2}(s,m_l^2,M_l^2)}{2\sqrt{s}}=\frac{\sqrt{s-(M_l+m_l)^2}\sqrt{s-(M_l-m_l)^2}}{2\sqrt{s}}, \tag{14}$$

with λ the triangular function.

Actually, the loop function in Eq. (11) can be calculated in the dimensional regularization without the on-shell approximation taken into account. Thus the loop function takes the form of

$$\begin{aligned} G_l=&\frac{\gamma_\mu P^\mu}{32P^2\pi^2}\left[(a_l+1)(m_l^2-M_l^2)+(m_l^2\ln\frac{m_l^2}{\mu^2}-M_l^2\ln\frac{M_l^2}{\mu^2})\right] \\ &+\left(\frac{\gamma_\mu P^\mu[P^2+M_l^2-m_l^2]}{4P^2M_l}+\frac{1}{2}\right)G_l'. \end{aligned} \tag{15}$$

Since the total three-momentum $\vec{P}=0$ in the center of mass frame, only the γ_0P^0 parts remain in Eq. (15). The external particles in the potential of the baryon and the meson in Eq. (7) are all on-shell, so the anti-particle is not included in the intermediate states when the Bethe-Salpeter equation is solved. Thus γ_0P^0 can be treated as the total energy of the system $P^0=\sqrt{s}$ in Eq. (15). Therefore, the loop function in Eq. (15) is simplified as

$$\begin{aligned} G_l=&\frac{\sqrt{s}}{32\pi^2 s}\left[(a_l+1)(m_l^2-M_l^2)+(m_l^2\ln\frac{m_l^2}{\mu^2}-M_l^2\ln\frac{M_l^2}{\mu^2})\right] \\ &+\left(\frac{s+M_l^2-m_l^2}{4M_l\sqrt{s}}+\frac{1}{2}\right)G_l'. \end{aligned} \tag{16}$$

Apparently, some off-shell corrections have been included in the revised form of the loop function in Eq. (16), which can be regarded as a kind of relativistic kinetic effect of the loop function.

Assuming the amplitudes near the pole to behave as

$$T_{ij}=\frac{g_ig_j}{z-z_R}, \tag{17}$$

with z_R the position of the pole on the complex $\sqrt{s}$ plane, and j and i being the initial and final channels, respectively, we can obtain the size of the coupling constants g_i by evaluating the residues of the diagonal elements T_{ii}. When the strongest coupled channel is determined, the coupling constants to the other channels, g_j, can be evaluated with the residues of the non-diagonal elements T_{ij} and the largest coupling constant g_i by using Eq. (17).

3 Experimental data and parameter fits

The energy shift and the width of the 1s state of kaonic hydrogen measured by the SIDDHARTA Collaboration are given as

$$\Delta E=283\pm36\pm6 \text{ eV}, \tag{18}$$

and

$$\Gamma=541\pm89\pm22 \text{ eV}, \tag{19}$$

respectively [16]. These results will constrain the parameter fit when the Bethe-Salpeter equation is solved.

In order to fit the experimental data at the K^-p threshold with the same formula as in Ref. [17], the potential of the baryon octet and the pseudoscalar meson in Eq. (7) has to be multiplied by a factor of $\sqrt{M_iM_j}$, where M_i and M_j denote the masses of the initial and final baryons, respectively, i.e.,

$$\tilde{V}_{ij}=V_{ij}\sqrt{M_iM_j}. \tag{20}$$

In the meantime, the loop function in Eq. (16) is divided by the mass of the intermediate baryon M_l, i.e.,

$$\tilde{G}_l=G_l/M_l. \tag{21}$$

Since the pole appears when the determinant $|1-VG|=0$, the modification in Eqs. (20) and (21) will not significantly affect the pole position on the complex $\sqrt{s}$ plane.

The forward scattering amplitude f_{ij} is related to the T-matrix,

$$f_{ij}(\sqrt{s})=\frac{1}{8\pi\sqrt{s}}\tilde{T}_{ij}(\sqrt{s}), \tag{22}$$

with $\tilde{T}=[1-\tilde{V}\tilde{G}]^{-1}\tilde{V}$, and the K^-p scattering length can be defined by the K^-p elastic scattering amplitude at threshold,

$$a(K^-p)=f_{11}(\sqrt{s}=M_{K^-}+m_p), \tag{23}$$

which is a complex number when the inelastic channels are taken into account.

The energy shift and width of the 1s state of kaonic hydrogen are related to the K^-p scattering length, which can be written as [27]

$$\Delta E-i\frac{1}{2}\Gamma=-2\alpha^3\mu_\gamma^2a(K^-p)[1+2\alpha\mu_\gamma(1-\ln\alpha)a(K^-p)], \tag{24}$$

with α the fine structure constant and $\mu_\gamma=\frac{m_{K^-}M_p}{m_{K^-}+M_p}$ the K^-p reduced mass.

Moreover, the branching ratios at the K^-p threshold are defined as

$$\gamma=\frac{\Gamma(K^-p\to\pi^+\Sigma^-)}{\Gamma(K^-p\to\pi^-\Sigma^+)}=\frac{\sigma_{51}}{\sigma_{61}}, \tag{25}$$

$$R_n=\frac{\Gamma(K^-p\to\pi^0\Lambda)}{\Gamma(K^-p\to\text{neutral states})}=\frac{\sigma_{31}}{\sigma_{31}+\sigma_{41}}, \tag{26}$$

and

$$R_c=\frac{\Gamma(K^-p\to\pi^+\Sigma^-,\pi^-\Sigma^+)}{\Gamma(K^-p\to\text{all inelastic channels})}=\frac{\sigma_{51}+\sigma_{61}}{\sigma_{51}+\sigma_{61}+\sigma_{31}+\sigma_{41}}, \tag{27}$$

respectively. All partial cross sections σ_{ij} are calculated at the K^-p threshold.

$$\sigma_{ij}=\frac{\bar{q}_i}{\bar{q}_j}\frac{\left|\tilde{T}_{ij}\right|^2}{16\pi s}, \tag{28}$$

where $\bar{q}_j$ and $\bar{q}_i$ are the three-momentum of the initial and final states in the center of mass frame, respectively.

The values of three branching ratios are taken from Ref. [28, 29], i.e.,

$$\gamma=2.36\pm0.04,\ R_n=0.189\pm0.015,\ R_c=0.664\pm0.011, \tag{29}$$

The subtraction constants a_l in Eq. (16) for different channels can be determined according to experimental data at the K^-p threshold, which are labeled Off-shell in Table I. Moreover, the corresponding subtraction constants in the original on-shell factorization approximation in Eq. (13) are also listed in Table 1, labeled On-shell [9].

Table 1. The subtraction constants used in the calculation with μ=630 MeV. The label Off-shell denotes the values for the loop function in Eq. (16), where some off-shell corrections are taken into account, while the label On-shell stands for those original values in the on-shell factorization approximation in Eq. (13) [9].

a_l	$\bar{K}N$	$\pi\Lambda$	$\pi\Sigma$	$\eta\Lambda$	$\eta\Sigma$	$K\Xi$
On-shell	−1.84	−1.83	−2.0	−2.25	−2.38	−2.67
Off-shell	−1.1	−1.6	−1.9	−2.7	−2.6	−2.8

The corresponding values of the energy shift ΔE and width Γ of the 1s state of kaonic hydrogen, and the branching ratios R_n and R_c defined in Eqs. (26) and (27) reproduced with the loop function in Eq. (16), are listed in Table 2. The subtraction constants labeled with Off-shell are used. These values are also calculated with the On-shell subtraction constants in the on-shell factorization approximation. The results show that the Off-shell subtraction constants fitted with the experiment data at the K^-p threshold are reasonable.

Table 2. The energy shift ΔE and width Γ of the 1s state of kaonic hydrogen, and the branching ratios R_n and R_c defined in Eqs. (26) and (27), calculated with different subtraction constant sets. The meanings of the labels On-shell and Off-shell are the same as in Table 1.

	ΔE/eV	Γ/eV	R_n	R_c
Experimental data	283±36±6	541±89±22	0.189±0.015	0.664±0.011
On-shell	−180.11	444.14	0.28	0.61
Off-shell	283.13	541.06	0.3	0.61

Since the meson-baryon amplitude T_{ij} is calculated in the isospin sectors, the subtraction constant a_{KN} is supposed to take the same value both in the K^-p channel and in the $\bar{K}^0n$ channel. Thus the branching ratio γ is always one in our calculation.

4 The isospin $I=0$ sector

We shall discuss the scattering amplitude in the isospin states, and thus we must use the average mass for the $\pi(\pi^+,\pi^0,\pi^-)$, $K(K^+,K^0)$, $\bar{K}(\bar{K}^0,K^-)$, $N(p,n)$, $\Sigma(\Sigma^+,\Sigma^0,\Sigma^-)$ and $\Xi(\Xi^0,\Xi^-)$ particles. There are four coupled states with isospin I=0 and strangeness S=−1, which are $\bar{K}N$, $\pi\Sigma$, $\eta\Lambda$ and $K\Xi$.

The phase conventions $|\pi^+\rangle=-|1,1\rangle$, $|K^-\rangle=-|\frac{1}{2},-\frac{1}{2}\rangle$, $|\Sigma^+\rangle=-|1,1\rangle$ and $|\Xi^-\rangle=-|\frac{1}{2},-\frac{1}{2}\rangle$ are used for the isospin states, which are consistent with the structure of the Φ and B matrices. The isospin state with $I=0$ can then be written as

$$\begin{aligned}|\bar{K}N,I=0\rangle&=\frac{1}{\sqrt{2}}(\bar{K}^0n+K^-p),\\ |\pi\Sigma,I=0\rangle&=-\frac{1}{\sqrt{3}}(\pi^+\Sigma^-+\pi^0\Sigma^0+\pi^-\Sigma^+),\\ |K\Xi,I=0\rangle&=-\frac{1}{\sqrt{2}}(K^0\Xi^0+K^+\Xi^-).\end{aligned} \tag{30}$$

The corresponding coefficients C_{ij} for the isospin states with $I=0$ are listed in Table B2. With these coefficients, the amplitudes T with isospin $I=0$ can be obtained by solving the Bethe-Salpeter equation in Eq. (10).

The squared amplitude $|T|^2$ in the $\pi\Sigma$ channel with isospin $I=0$ on the complex $\sqrt{s}$ plane is shown in Fig. 1. Some poles are generated dynamically when the Bethe-Salpeter equation is solved in the unitary coupled-channel approximation. In Fig. 1, the poles generated

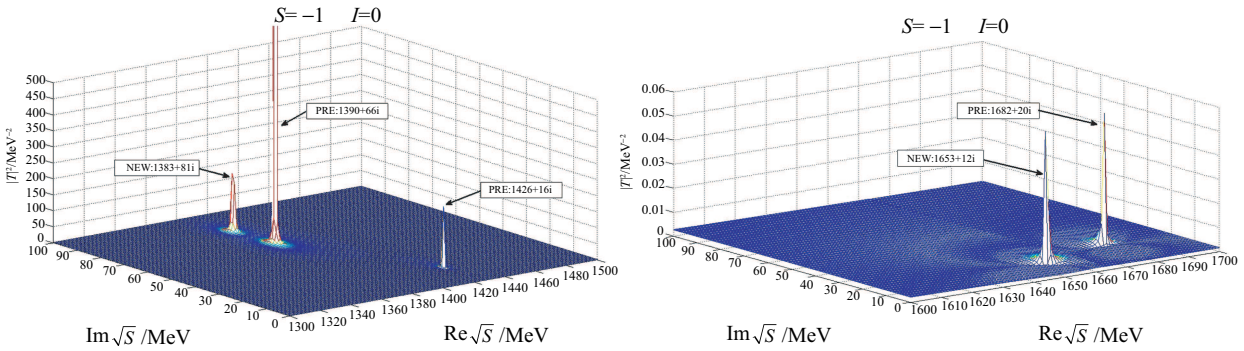

Fig. 1. Comparison of poles in the strangeness $S=-1$ and isospin $I=0$ sector. NEW denotes the case calculated from the loop function in Eq. (16), while PRE stands for the case of the loop function in the on-shell factorization approximation in Eq. (13).

dynamically with the loop function in Eq. (16) are labeled with NEW, while the label PRE denotes the poles generated with the loop function in the on-shell factorization in Eq. (13).

Table 3. Coupling constants to meson-baryon states in the isospin $I=0$ sector. The label NEW denotes the case calculated from the loop function in Eq. (16), while the label PRE stands for the case of the loop function in the on-shell factorization approximation in Eq. (13).

	PRE		NEW	
z_R	$1390+66i$		$1383+81i$	
$(I=0)$	g_i	$\lvert g_i\rvert$	g_i	$\lvert g_i\rvert$
$\pi\Sigma$	$-2.5-1.5i$	2.9	$-2.1-1.5i$	2.5
$\bar{K}N$	$1.2+1.7i$	2.1	$0.8+0.8i$	1.1
$\eta\Lambda$	$0.0+0.8i$	0.8	$-0.1+0.2i$	0.24
$K\Xi$	$-0.5-0.4i$	0.6	$-0.4-0.5i$	0.6
	PRE		NEW	
z_R	$1426+16i$		–	
$(I=0)$	g_i	$\lvert g_i\rvert$	g_i	$\lvert g_i\rvert$
$\pi\Sigma$	$0.4-1.4i$	1.5	–	–
$\bar{K}N$	$-2.5+0.9i$	2.7	–	–
$\eta\Lambda$	$-1.4+0.2i$	1.4	–	–
$K\Xi$	$0.1-0.3i$	0.4	–	–
	PRE		NEW	
z_R	$1680+20i$		$1653+12i$	
$(I=0)$	g_i	$\lvert g_i\rvert^2$	g_i	$\lvert g_i\rvert^2$
$\pi\Sigma$	$-0.0-0.3i$	0.3	$-0.1-0.3i$	0.3
$\bar{K}N$	$0.3+0.7i$	0.8	$-0.0+0.7i$	0.7
$\eta\Lambda$	$-1.1-0.1i$	1.1	$-1.1+0.2i$	1.1
$K\Xi$	$3.4+0.1i$	3.5	$3.0-0.1i$	3.0

In the energy region near 1400 MeV, only one pole is generated dynamically in the isospin $I=0$ sector, located at $1383+81i$ MeV on the complex $\sqrt{s}$ plane. This pole is higher than the $\pi\Sigma$ threshold and lies in the second Riemann sheet, and thus it can be regarded as a counterpart of the $\Lambda(1405)$ particle in the Particle Data Group (PDG) data [30]. Actually, another peak is generated dynamically, at $1435+2i$ MeV on the complex $\sqrt{s}$ plane. However, it is too low to be detected in Fig. 1. Apparently, when the off-shell correction of the loop function in the Bethe-Salpeter equation is taken into account, the peak near the $\bar{K}N$ threshold is suppressed strongly, and only one pole is detected in the region of 1400 MeV. The resonance at $1383+81i$ MeV couples strongly to the $\pi\Sigma$ channel. In the $\bar{K}N$, $\eta\Lambda$ and $K\Xi$ channels, the cases are similar to that in the $\pi\Sigma$ channel, and only one pole can be found clearly. Furthermore, there is another pole at $1653+12i$ MeV generated dynamically on the complex $\sqrt{s}$ plane, lower than the $\eta\Lambda$ threshold, and lying in the third Riemann sheet. The pole at the position of $\sqrt{S}=1653+12i$ MeV can be regarded as a candidate for the $\Lambda(1670)1/2^-$ resonance, which couples strongly to the $K\Xi$ channel.

Their coupling constants to different meson-baryon states are listed in Table 3, where the label New denotes the results with the loop function in Eq. (16), while the label PRE means the results calculated with the loop function in the on-shell factorization, as in Eq. (13).

5 The isospin $I=1$ sector

In the isospin $I=1$ sector, we have five coupled states, $\bar{K}N$, $\pi\Sigma$, $\pi\Lambda$, $\eta\Sigma$ and $K\Xi$.

The isospin state with $I=1$ can be written as

$$\begin{aligned}|\bar{K}N,I=1\rangle&=\frac{1}{\sqrt{2}}(\bar{K}^0n-K^-p),\\ |\pi\Sigma,I=1\rangle&=\frac{1}{\sqrt{2}}(\pi^-\Sigma^+-\pi^+\Sigma^-),\\ |K\Xi,I=1\rangle&=\frac{1}{\sqrt{2}}(K^0\Xi^0-K^+\Xi^-).\end{aligned}\tag{31}$$

The coefficients C_{ij} for the isospin states with $I=1$ can be constructed by using Eq. (31) and Table B1, and are given in Table B3.

There is only one peak of squared amplitudes $|T|^2$ detected at $1570+i244$ MeV on the complex $\sqrt{s}$ plane. It

is lower than the $\eta\Sigma$ threshold and lies in the fourth Riemann sheet. The resonance at $1570+i244$ MeV is similar to the $\Sigma(1580)3/2-$ state in the PDG data. Nevertheless, in the S-wave approximation, the total angular momentum of the resonance at $1570+i244$ MeV is $J=1/2$, and its parity is negative. Furthermore, its decay width is too large, so it apparently cannot be $\Sigma(1580)3/2-$. The resonance at $1570+i244$ MeV is more possible to correspond to the $\Sigma(1620)1/2-$ state in the PDG data, although its mass is lower about 50 MeV than the latter. From Table 4, we know that this resonance couples strongly to the $K\Xi$ channel.

Table 4. Same as Table 3 but for the isospin $I=1$ sector.

	PRE		NEW	
z_R	$1579+264i$		$1570+244i$	
$(I=1)$	g_i	$\lvert g_i\rvert^2$	g_i	$\lvert g_i\rvert^2$
$\pi\Lambda$	$1.4+1.5i$	2.0	$1.3+1.4i$	1.9
$\pi\Sigma$	$-2.2-1.5i$	2.7	$-2.2-1.2i$	2.5
$\bar{K}N$	$-1.1-1.1i$	1.6	$-1.0-1.2i$	1.6
$\eta\Sigma$	$1.2+1.4i$	1.9	$1.1+1.3i$	1.7
$K\Xi$	$-2.5-2.4i$	3.5	$-2.4-2.1i$	3.2

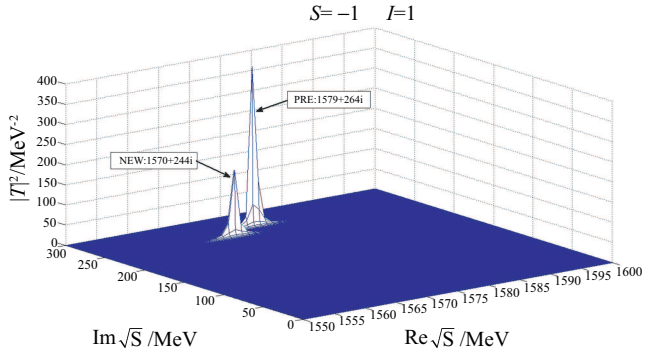

Fig. 2. Same as Fig. 1 but for the strangeness $S=-1$ and isospin $I=1$ sector.

The squared amplitude $|T|^2$ in the $\pi\Sigma$ channel with strangeness $S=-1$ and isospin $I=1$ as a function of the total energy $\sqrt{s}$ in the center of mass frame is depicted in Fig. 2, where the label PRE denotes the results calculated with the loop function in the on-shell factorization, and the label NEW means those of the loop function in Eq. (16). The pole positions are different in these two schemes.

6 Discussion and conclusion

In this article, the formula of the loop function in the Bethe-Salpeter equation is deduced in the dimensional regularization scheme. Compared with the loop function in the on-shell factorization approximation, the relativistic kinetic effect and off-shell corrections are taken into account in the revised scheme.

The interaction between the pseudoscalar meson and the baryon is studied in the strangeness $S=-1$ sector. According to the experimental data at the K^-p threshold, the subtraction constants of the loop function in the Bethe-Salpeter equation are determined, and some resonances are generated dynamically in the unitary coupled-channel approximation. When the off-shell correction of the loop function is taken into account, the squared amplitude is suppressed strongly, and only one resonance peak is detected in the 1400 MeV region, which is above the $\pi\Sigma$ threshold and is assumed to be associated with the $\Lambda(1405)$ particle. Moreover, the coupling constants of the resonance to meson-baryon states are similar to the corresponding states in Ref. [7], and the resonance in the 1400 MeV region couples strongly with the $\pi\Sigma$ channel.

We would like to thank Han-Qing Zheng, Eulogio Oset and En Wang for useful discussions.

Appendix A

A loop function in the dimensional regularization scheme

In the dimensional regularization scheme, the loop function in the Bethe-Salpeter equation can be deduced according to the Passarino-Veltman procedure [31],

$$G_l(s)=i\int\frac{\mathrm{d}^4q}{(2\pi)^4}\frac{\not{q}+M_l}{q^2-M_l^2+i\epsilon}\frac{1}{(P-q)^2-m_l^2+i\epsilon}=-\not{P}A(s)+\frac{1}{2}G'(s), \tag{A1}$$

where

$$\begin{aligned}G'(s) &= i\int\frac{\mathrm{d}^4q}{(2\pi)^4}\frac{2M_l}{q^2-M_l^2+i\epsilon}\frac{1}{(P-q)^2-m_l^2+i\epsilon}\\ &= \frac{2M_l}{16\pi^2}\left\{a_l+\ln\frac{M_l^2}{\mu^2}+\frac{m_l^2-M_l^2+s}{2s}\ln\frac{m_l^2}{M_l^2}+\frac{\bar{q}_l}{\sqrt{s}}\left[\ln(s-(M_l^2-m_l^2)+2\bar{q}_l\sqrt{s})+\ln(s+(M_l^2-m_l^2)+2\bar{q}_l\sqrt{s})\right.\right.\\ &\quad\left.\left.-\ln(-s+(M_l^2-m_l^2)+2\bar{q}_l\sqrt{s})-\ln(-s-(M_l^2-m_l^2)+2\bar{q}_l\sqrt{s})\right]\right\},\end{aligned} \tag{A2}$$

and

$$P^\mu A(s) = -i\int \frac{\mathrm{d}^4q}{(2\pi)^4}\frac{q^\mu}{q^2-M_l^2+i\epsilon}\frac{1}{(P-q)^2-m_l^2+i\epsilon}.$$

Since $-2P\cdot q = [(P-q)^2-m_l^2]-[q^2-M_l^2]+m_l^2-M_l^2-P^2$,

$$\begin{aligned}
-2P^2A(s) &= -i\int \frac{\mathrm{d}^4q}{(2\pi)^4}\frac{-2P\cdot q}{q^2-M_l^2+i\epsilon}\frac{1}{(P-q)^2-m_l^2+i\epsilon}\\
&= -i\int \frac{\mathrm{d}^4q}{(2\pi)^4}\frac{[(P-q)^2-m_l^2]-[q^2-M_l^2]+m_l^2-M_l^2-P^2}{[q^2-M_l^2+i\epsilon][(P-q)^2-m_l^2+i\epsilon]}\\
&= -i\int \frac{\mathrm{d}^4q}{(2\pi)^4}\frac{1}{q^2-M_l^2+i\epsilon}-i\int \frac{\mathrm{d}^4q}{(2\pi)^4}\frac{-1}{(P-q)^2-m_l^2+i\epsilon}-i\int \frac{\mathrm{d}^4q}{(2\pi)^4}\frac{m_l^2-M_l^2-P^2}{[q^2-M_l^2+i\epsilon][(P-q)^2-m_l^2+i\epsilon]}\\
&= -\frac{M_l^2}{16\pi^2}\left(1+a_l+\ln(\frac{M_l^2}{\mu})\right)+\frac{m_l^2}{16\pi^2}\left(1+a_l+\ln(\frac{m_l^2}{\mu})\right)-\frac{(P^2+M_l^2-m_l^2)}{2M_l}(-G'(s)).
\end{aligned}$$

Thus the formula of $A(s)$ can be written as

$$A(s)=\frac{1}{-2P^2}\left\{-\frac{M_l^2}{16\pi^2}\left(1+a_l+\ln(\frac{M_l^2}{\mu})\right)+\frac{m_l^2}{16\pi^2}\left(1+a_l+\ln(\frac{m_l^2}{\mu})\right)-\frac{(P^2+M_l^2-m_l^2)}{2M_l}(-G'(s))\right\}, \tag{A3}$$

with $P^2=s$.

By replacing the $G'(s)$ and $A(s)$ in Eq. (A1) with Eqs. (A2) and (A3), respectively, the formula of the loop function in Eq. (15) is obtained.

Appendix B

The coefficients C_{ij} in the pseudoscalar meson-baryon octet interaction in the $S=-1$ channel

Table B1. The coefficients C_{ij} in the pseudoscalar meson-baryon octet interaction in the $S=-1$ channel, $C_{ij}=C_{ji}$.

	K^-p	$\bar{K}^0n$	$\pi^0\Lambda$	$\pi^0\Sigma^0$	$\eta\Lambda$	$\eta\Sigma^0$	$\pi^+\Sigma^-$	$\pi^-\Sigma^+$	$K^+\Xi^-$	$K^0\Xi^0$
K^-p	2	1	$\frac{\sqrt{3}}{2}$	$\frac{1}{2}$	$\frac{3}{2}$	$\frac{\sqrt{3}}{2}$	0	1	0	0
$\bar{K}^0n$		2	$-\frac{\sqrt{3}}{2}$	$\frac{1}{2}$	$\frac{3}{2}$	$-\frac{\sqrt{3}}{2}$	1	0	0	0
$\pi^0\Lambda$			0	0	0	0	0	0	$\frac{\sqrt{3}}{2}$	$-\frac{\sqrt{3}}{2}$
$\pi^0\Sigma^0$				0	0	0	2	2	$\frac{1}{2}$	$\frac{1}{2}$
$\eta\Lambda$					0	0	0	0	$\frac{3}{2}$	$\frac{3}{2}$
$\eta\Sigma^0$						0	0	0	$\frac{\sqrt{3}}{2}$	$-\frac{\sqrt{3}}{2}$
$\pi^+\Sigma^-$							2	0	1	0
$\pi^-\Sigma^+$								2	0	1
$K^+\Xi^-$									2	1
$K^0\Xi^0$										2

Table B2. The coefficients C_{ij} for the isospin states with I=0, C_{ij}=C_{ji}.

	$\bar{K}N$	$\pi\Sigma$	$\eta\Lambda$	$K\Xi$
$\bar{K}N$	3	$-\sqrt{\frac{3}{2}}$	$\frac{3}{\sqrt{2}}$	0
$\pi\Sigma$		4	0	$\sqrt{\frac{3}{2}}$
$\eta\Lambda$			0	$-\frac{3}{\sqrt{2}}$
$K\Xi$				3

Table B3. The coefficients C_{ij} for the isospin states with I=1, C_{ij}=C_{ji}.

	$\bar{K}N$	$\pi\Sigma$	$\pi\Lambda$	$\eta\Sigma$	$K\Xi$
$\bar{K}N$	1	-1	$-\sqrt{\frac{3}{2}}$	$-\sqrt{\frac{3}{2}}$	0
$\pi\Sigma$		2	0	0	1
$\pi\Lambda$			0	0	$-\sqrt{\frac{3}{2}}$
$\eta\Sigma$				0	$-\sqrt{\frac{3}{2}}$
$K\Xi$					1

References

1 R. H. Dalitz and S. F. Tuan, Ann. Phys. (N. Y.) **10**: 307 (1960)
2 R. H. Dalitz, T. C. Wong, G. Rajasekaran, Phys. Rev., **153**: 1617 (1967)
3 L. S. Kisslinger and E. M. Henley, Eur. Phys. J. A, **47**: 8 (2011)
4 I. Zychor et al, Phys. Lett. B, **660**: 167 (2008)
5 N. Isgur and G. Karl, Phys. Rev. D, **18**: 4187 (1978)
6 J. A. Oller, U.-G Meißner, Phys. Letter. B, **500**: 263 (2001)
7 D. Jido, J. A. Oller, E. Oset, A. Ramos. U.-G Meißner, Nuclear Physics A, **725**: 181 (2003)
8 L. S. Geng and E. Oset, Eur. Phys. J. A, **34**: 405 (2007)
9 E. Oset, A. Ramos, C. Bennhold. Phys. Lett. B, **527**: 99 (2002); E. Oset, A. Ramos, C. Bennhold. Erratum, Phys. Lett. B, **530**: 260 (2002)
10 T. Hyodo, A. Hosaka, E. Oset, A. Ramos, and M. J. Vicente Vacas, Phys. Rev. C, **68**: 065203 (2003)
11 A. Cieply and J. Smejkal, Eur. Phys. J. A, **43**: 191 (2010)
12 M. Hassanvand et al, Phys Rev. C, **87**: 055202 (2013)
13 R. H. Dalitz and A. Deloff. J. Phys. G, **17**: 289 (1991)
14 G. Alexander, G. R. Kalbfleisch, D. H. Miller et al, Phys. Rev. Lett., **8**: 447 (1962)
15 K. Moriya et al (CLAS Collaboration), Phys. Rev. C, **87**(3): 035206 (2013)
16 M. Bazzi et al (SIDDHARTA Collaboration), Phys. Lett. B, **704**: 113 (2011)
17 Y. Ikeda, T. Hyodo, and W. Weise, Nucl. Phys. A, **881**: 98 (2012)
18 M. Mai and U. G. Meißner, Nucl. Phys. A, **900**: 51 (2013)
19 Z. H. Guo and J. A. Oller, Phys. Rev. C, **87**(3): 035202 (2013)
20 M. Mai and U. G. Meißner, Eur. Phys. J. A, **51**(3): 30 (2015)
21 A. Cieply, M. Mai, U. G. Meißner, and J. Smejkal, Nucl. Phys. A, **954**: 17 (2016)
22 A. Pich, Rep. Prog. Phys., **58**: 563 (1995)
23 G. Ecker, Prog. Part. Nucl. Phys., **35**: 1 (1995)
24 V. Bernard, N. Kaiser, and U. G. Meißner, Int. J. Mod. Phys. E, **4**: 193 (1995)
25 P. C. Bruns, M. Mai, and U. G. Meißner, Phys. Lett. B, **697**: 254 (2011)
26 E. Oset, A. Ramos, Nucl. Phys. A, **635**: 99 (1998)
27 U. G. Meißner, U. Raha, and A. Rusetsky, Eur. Phys. J. C, **35**: 349 (2004)
28 D. N. Tovee et al, Nucl. Phys. B, **33**: 493 (1971)
29 R. J. Nowak et al, Nucl. Phys. B, **139**: 61 (1978)
30 K. A. Olive et al (Particle Data Group), Chin. Phys. C, **38**: 090001 (2014)
31 G. Passarino and M. J. G. Veltman, Nucl. Phys. B, **160**: 151 (1979)